Applied Acoustics 213 (2023) 109624

Contents lists available at ScienceDirect

Applied Acoustics

journal homepage: www.elsevier.com/locate/apacoust

Parametric analysis of acoustically levitated droplet for potential microgravity application

Aditya Vashi, Ajeet Singh Yadav, Nam-Trung Nguyen, Kamalalayam Rajan Sreejith *

Queensland Micro and Nanotechnology Centre, Griffith University, 170 Kessels Road, Nathan 4111, QLD, Australia

ARTICLE INFO

Keywords:
Acoustic levitation
Internal flow
Droplet shape
Microgravity
Clinostat
Digital microfluidics

ABSTRACT

Acoustic levitation is a versatile technique for the non-contact handling of both solid and liquid samples, yet its potential remains underutilized in container-less processing and lab-on-a-drop application. This study demonstrates the efficient use of acoustically levitated droplets as microgravity simulators on earth similar to clinostat. Using a simple and affordable non-resonant single-axis acoustic levitator called TinyLev, we first investigate the impact of applied voltage and droplet volume on the shape and rotational motion of levitated water droplets. Furthermore, we examine the rotational motion of suspended microparticles within the droplets. Our findings reveal the feasibility of using the levitated droplets as a miniaturized microgravity simulators on earth.

1. Introduction

Levitation involves suspending solid particles or fluid droplets in the air or another medium to counteract gravity. This technique offers numerous advantages in container-less processing [1,2] and lab-on-a-drop applications [3,4]. The concept has found applications in material science [5], analytical chemistry [6], fluid dynamics [7], and biophysics [8]. Levitation can be achieved through optical [9], acoustic [10], magnetic [11], aerodynamic [12], and electrostatic [13] forces [14]. However, optical and aerodynamic levitation requires expensive and sophisticated equipment, while electrostatic levitation is limited to electrically charged samples. Magnetic levitation requires a high magnetic field and magnetic objects. In contrast, acoustic levitation can levitate any type of materials without a specific property [15]. Acoustic levitators with a single-axis configuration are commonly used for acoustic levitation. They are categorized as resonant [16] or non-resonant [17]. Resonant levitators use an acoustic emitter and reflector to create a standing wave at resonance, whereas non-resonant levitators use emitters on both sides to generate the standing wave without requiring distance tuning.

Digital microfluidic platforms have gained importance in the rapidly growing field of microfluidics. Common platforms include liquid drops, liquid marbles, and core–shell beads [18,19]. Liquid marbles consist of liquid droplets covered with a hydrophobic powder, while core–shell beads have a solid shell surrounding a liquid droplet. The ability to acoustically levitate these platforms provide an opportunity to investigate their dynamics, such as equilibrium shape [20,21], internal flow [22–24], and oscillation [25,26]. This capability of acoustically levitated digital microfluidics platforms has found applications in crystallisation [27], self-assembly [28], material solidification [29] and biochemical reaction [24,30]. However, the potential of acoustically levitated digital microfluidic platforms to simulate microgravity on earth remains unexplored. The simplicity, affordability, and compact nature of basic acoustic levitation systems make them suitable for non-contact container-less liquid sample handling and microgravity simulation.

This paper reports the investigation of acoustically levitated droplet as a clinostat and simulate microgravity on Earth. A clinostat is simple and widely used microgravity simulator [31], which takes advantage of the rotational motion to neutralize gravity's effects on samples [32]. We use commercially available less expensive and simple non-resonant single-axis acoustic levitator known as TinyLev for this study [33]. The research is divided into two parts. First, we focused on analysing the influence of driving voltage and droplet volume on the droplet's shape. We quantified the shape change by evaluating the aspect ratio of the levitated droplet. Next, we studied the rotational motion of a suspended microparticle within the levitated droplet. We examine the effect of applied voltage and droplet volume on the particle's rotation and determine the ratio of centrifugal acceleration to gravitational acceleration to assess the microgravity conditions experienced by the

* Corresponding author.
E-mail addresses: aditya.vashi@griffithuni.edu.au (A. Vashi), ajeet.yadav@griffithuni.edu.au (A.S. Yadav), nam-trung.nguyen@griffith.edu.au (N.-T. Nguyen), s.kamalalayamrajan@griffith.edu.au (K.R. Sreejith).

https://doi.org/10.1016/j.apacoust.2023.109624
Received 5 June 2023; Received in revised form 1 August 2023; Accepted 30 August 2023

suspended microparticle.

2. Theory

2.1. Acoustic pressure and shape change in a levitated liquid droplet

The proposed project will utilise a single-axis non-resonant type acoustic levitator. The acoustic force exerted on a spherical droplet levitated in an acoustic field can be represented as the negative gradient of Gor'kov potential [34],

$$F = -\nabla U. \tag{1}$$

The Gor'kov potential in the complex acoustic pressure field p is given as,

$$U = 2K_1|p|^2 - 2K_2|p_x|^2 + 2K_2|p_y|^2 + 2K_2|p_z|^2 \tag{2}$$

where,

$$K_1 = \frac{1}{4v\left(\frac{1}{\rho_0 c_0^2} - \frac{1}{\rho_p c_p^2}\right)} \tag{3}$$

and,

$$K_2 = \frac{3}{4}v\left(\frac{\rho_0 - \rho_p}{\omega^2\rho_0(\rho_0 + \rho_p)}\right) \tag{4}$$

where v is the volume of the droplet, ρ_0 and ρ_p are the densities of the hosting medium and the levitated droplet respectively, ω is the frequency of the ultrasonic wave. c_0 and c_p are the speed of the wave through the hosting medium and the levitated droplet. p_x, p_y, and p_z are the derivatives of the pressure p in the x, y and z directions, respectively. From the equations, it is evident that the effect of acoustic radiation force on a levitating droplet varies with its volume if other liquid properties remain unchanged. It should also be noted that the acoustic pressure field at any point r from the source of sound is represented as [35],

$$p(\mathrm{r}) = p_0 V\left((D_f(q)/d)e^{i(\varphi + kd)}\right) \tag{5}$$

where V is the applied voltage to the levitator, D_f is the directivity function which depends on the angle q between the normal to the source of sound and r, d is the propagation distance in space, φ is the emitting phase of the source and, k is the wave number. The wave number k is related to the wavelength λ of the sound wave by the equation, $k = \frac{2\pi}{\lambda}$. This fundamental theory applies directly to a levitating droplet. The equations pertaining to acoustic levitation outlined above have led to the hypothesis that increasing the applied voltage to the levitator results in an amplified acoustic pressure exerted on levitated droplets. Consequently, this amplified acoustic pressure deforms the levitated droplet, which results in non-spherical drop.

2.2. Rotational motion of acoustically levitated droplet and clinorotation

Apart from acoustic radiation force, acoustic streaming is another nonlinear effect which affects the levitated droplet. Acoustic streaming impacts the levitated droplet's internal and external flow fields. Rednikov et al. analytically investigated internal flow of the levitated droplet and found four recirculation zones within the droplet [36]. Trinh and Wang reported similar four-cell pattern inside the droplet during their study on oscillation [37]. However, they observed the rotation of levitated droplets around the horizontal axis once the oscillation attains certain amplitude [37]. This rotation is due to misalignment between the vertical axes of the droplet and the levitator leading to net acoustic torque on levitated droplet [38,39]. The torque acting on the droplet can be represented as,

$$\tau = F.d \tag{6}$$

where F is the resultant acoustic force and d is the length of the major axis of the droplet. Rotation of levitated droplet breaks symmetry of four-cell pattern inside droplet and gives rise to single forced vortex. This type of flow structure is also reported in articles [38,40]. Due to rotation and single vortex flow structure, a microparticle suspended in the droplet would experience a rotation inside the droplet. The centrifugal acceleration of the suspended particle in a rotating droplet can be represented as,

$$a_c = r\omega^2 \tag{7}$$

where ω is the angular velocity of the particle in rad/s and r is the radius of the droplet. The same can also be represented as:

$$\omega = \frac{\pi\omega_{rpm}}{30} \tag{8}$$

Substituting Eq. (8) in (7) and taking the ratio of centrifugal acceleration of the rotating particle to the gravitational acceleration gives

$$\frac{a_c}{g} = 1.12r\omega_{rpm}^2 \times 10^{-3} \tag{9}$$

The ratio of accelerations depends on the droplet's radius and angular velocity. When this ratio exceeds 1, the centrifugal force dominates, causing particles to experience a net outward force and move away from the centre of rotation. Conversely, when the ratio is below 1, particles move towards the centre, counteracting both centrifugation and sedimentation. However, when the ratio equals 1, the two forces balance each other, resulting in a state of weightlessness or microgravity as particles rotate in a circular motion without moving towards or away from the centre. To simulate microgravity, the clinostat maintains this ratio below 10^{-3}. In our experiments, we will investigate the influence of droplet volume and applied voltage on ω_{rpm} and endeavour to simulate a state of near microgravity in acoustically levitated droplets.

3. Materials and methods

3.1. Experimental setup

Fig. 1a illustrates the schematic of the experimental setup. The central component of the setup is the TinyLev acoustic levitator [33], which is fabricated using 3D printing technology. The TinyLev model incorporates 72 Manorshi ultrasonic transducers, with 36 transducers positioned on each side. These transducers, measuring 10 mm in diameter, operate at a frequency of 40 kHz and convert electrical energy into acoustic energy. They are arranged in a concentric circular pattern, with a spacing of 12 mm between each transducer. The overall packing radius of the circular configuration is 4.5 cm. The transducers are mounted on two circular curved plates, which are 11 cm apart from each other. The curvature enhances the trapping force at the focal point. To excite the transducers, a square wave is generated using a nano Arduino, which is then amplified by the L297N dual H-bridge stepper motor driver. The TinyLev device is powered by a variable DC power supply (Keithley 2200–30-5).

For visual observation of the levitated object, a high-speed front camera (XIMEA USB 3.0 1.3 MP B/W) with an Edmund Optics 1.0 × SilverTLTM Telecentric lens, as well as a side camera (XIMEA USB 3.0 1.3 MP RGB) with an Edmund Optics VZMTM 450 Zoom Imaging lens, are employed. The cameras are connected to laptops, capturing 2,000 frames at a rate of 100 frames per second (FPS). To enhance image quality, white light sources are affixed to the back and side of the TinyLev model.

3.2. Experimental procedure

Deionized water, combined with green, fluorescent polyethylene

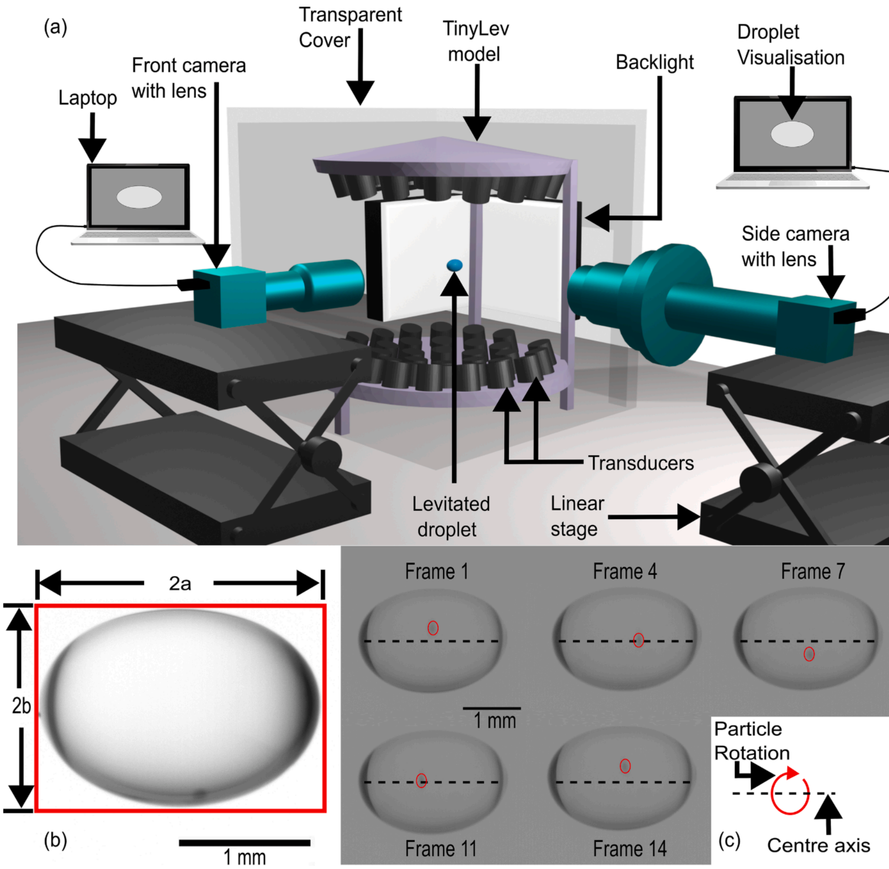

Fig. 1. (a) Experimental setup. (b) Measurement of length of major and minor axis using bounding box tool in python (front camera). (c) Measurement of angular velocity from picture frames (side camera).

microspheres (Cospheric, 27–32 µm, 1.00 g/cc), served as the working liquid for the experiment. Using a micropipette (Eppendorf Research, 1–20 µl), droplets with volumes of 5, 10, and 15 µl, each containing a single microparticle, were precisely positioned at the centre of the levitator cavity. To minimize disturbances caused by air, a transparent cover was applied to the levitator after successful droplet levitation. Videos were recorded to capture the behaviour of the levitated droplets. Voltage variations were introduced, ranging from 7.5 V to 9 V in increments of 0.5 V, and each experiment was conducted five times. The impact of voltage on the droplets was assessed by analysing the aspect ratio (a/b) of the levitated droplets. Where *a* and *b* are the lengths of the semimajor and semi-minor axis of the droplet. The bounding box toolbox in Python was used to find out *a* and *b* from the images (Fig. 1b). Moreover, from the measured aspect ratio, sound pressure can be evaluated with Marston's work on equilibrium shape of the levitated droplet [41]. For a given aspect ratio (a/b), sound pressure can be calculated as,

$$p = \sqrt[2]{\frac{\left(\frac{a}{b}-1\right)}{\left(\frac{2a}{b}-1\right)\left(\frac{3R}{64\sigma_p\rho_p c_0^2}\right)\left(1+\frac{7}{5}(kR)^2\right)}} \tag{10}$$

Table 1
Parameters to compute sound pressure.

Parameter	Value
Surface tension of water (σ_p)	0.072 N/m
Density of water (ρ_p)	997 kg/m^3
Speed of sound (c_0)	343 m/s
Wavenumber ($k = \frac{2\pi}{\lambda}$)	732.3 m^{-1}

where, *R* is the equatorial radius of the drop, and σ_p is the surface tension of levitated droplet. The parameters to compute the pressure is shown in Table 1.

The shortest radius of the rotating microparticle from the horizontal axis of the levitated droplet was measured to calculate the minimum microgravity experienced by the particle (Fig. 1c). The angular velocity of the particle is calculated by the equation,

$$\omega_{\text{rpm}} = \frac{60}{t} \tag{11}$$

where,

$$t = \frac{\text{Number of frames for one rotation}}{\text{frames per second set in the camera}} \tag{12}$$

4. Results and discussions

4.1. Simulation of acoustic field

Visualisation of the acoustic pressure field generated by transducers can be done with Levitate toolbox developed in Python language [42]. We simulated the TinyLev design according to its geometries. Fig. 2a and b shows the acoustic pressure distribution of the levitation at 10 V and 20 V respectively. The results of the simulation emphasise the effect of applied voltage on the shape of the droplet since the acoustic pressure shows a clear increase with applied voltage.

4.2. Effect of applied voltage and the volume on the shape of the levitated droplet

Fig. 3 illustrates the characteristics of acoustically levitated droplet.

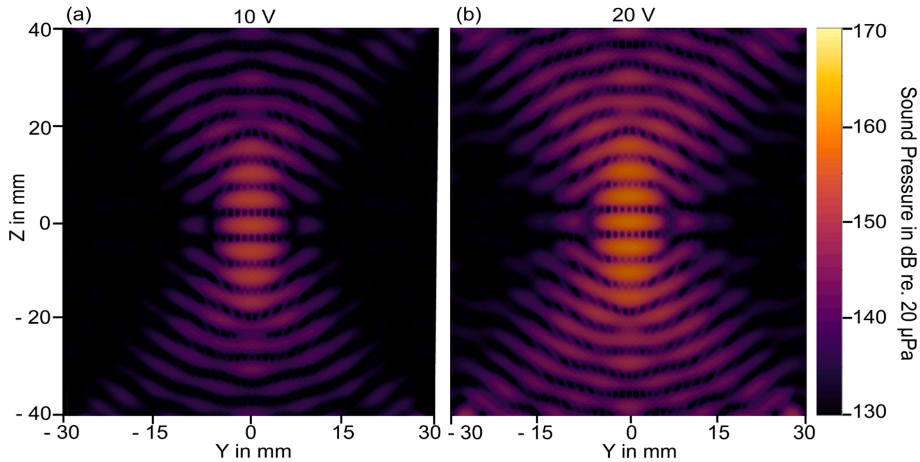

Fig. 2. Simulated sound pressure distribution for TinyLev at (a) 10 V and (b) 20 V.

Data points are fitted with suitable fitting curves. Fig. 3a shows that the aspect ratio of the levitated droplet increases as the applied voltage is increased. This is because the increased voltage leads to higher acoustic pressure on the droplet. The percentage increase in aspect ratio from 7.5 V to 9.0 V is 7.16 % for a 5 μl droplet, 11.86 % for a 10 μl droplet, and 7.64 % for a 15 μl droplet. The effect of increased voltage is more significant for smaller droplets, where the surface tension dominates, and the droplet tends to be nearly spherical. As the acoustic pressure increases, the droplet becomes compressed and takes on an elliptical shape, which is more noticeable with higher acoustic pressure. In larger droplets, where the gravitational force is already dominant, the increase in aspect ratio is less pronounced with increased voltage.

In Fig. 3b, it is evident that the aspect ratio of the droplet increases with volume at a particular voltage. This is because larger-volume droplets experience a stronger gravitational force. The percentage increase in aspect ratio from 5 μl to 15 μl for voltages 7.5 V, 8.0 V, 8.5 V, and 9.0 V is 10.4%, 21.7%, 18.1%, and 9.9% respectively. Therefore, both volume and applied voltage contribute to the shape of a levitated droplet. Sound pressure at any node can be calculated from the aspect ratio of the levitated droplet using Eq. (10). Fig. 3c shows the relationship between voltage and acoustic pressure at a particular node. The acoustic pressure increases with voltage like what was observed in the simulation. The percentage increase in acoustic pressure from 7.5 V to 9.0 V is 16.6%.

4.3. Effect of applied voltage and the volume on flow dynamics of the levitated droplet

Fig. 3d illustrates the relationship between the angular velocity of the dispersed microparticle and volume at a constant voltage. It is evident that the angular velocity decreases with increasing volume. This reduction is attributed to the inertia of larger droplets. The decrease in angular velocity from 5 μl to 15 μl for voltages 7.5 V, 8.0 V, 8.5 V, and 9.0 V is 63.3, 51.7, 49.8, and 51.3% respectively. This trends of the results of our study agree with the results of the study of Saha et al. [38] and Yan et al. [40], however more insight into this relation can be a scope of future study.

In Fig. 3e, the relationship between the angular velocity of the microparticle and the applied voltage is presented. The results indicate that the impact of voltage on the angular velocity is minimal. Despites the increase in applied acoustic pressure with voltage, the resultant force (F in Eq. (6)) experiences negligible changes. The change in acoustic pressure with voltage has significantly deformed the droplet, however this change is not enough to change the angular velocity of the droplet. The change in angular velocity for droplet volumes of 5 μl, 10 μl, and 15 μl is 1.2%, 4.3%, and 30.8% respectively, as the voltage ranges from 7.5 V to 9.0 V. The magnitude of variation in the rotation is more significant for larger volumes due to the higher value of d in those droplets. Increased d value combined with the negligible increase in F value accounts for the observed effect. From the experimental findings, it can be concluded that the effect of droplet volume on angular velocity is more pronounced than the influence of applied voltage.

The Supplementary videos S1 (front camera) and S2 (side camera) provide visual evidence of the rotation of particles within the levitated droplet. As time progresses, the particles exhibited a cyclic motion, moving towards and away from the droplet's centre. The particle was supposed to be rotating at a stable position from the horizontal axis. However, due to air perturbations, the levitated droplet experiences slight oscillations, causing the internal flow to influence the particle's displacement away from the centre. This phenomenon explains the observed cyclic movement along the horizontal axis.

To quantify the relationship between centrifugal acceleration and gravity, the smallest radius of rotation of the particle from the droplet's centre was measured. By utilizing Eq. (10), the ratio of centrifugal acceleration a_c to gravitational acceleration g is calculated for different voltages and volumes. Fig. 3f illustrates that the lowest value of $\frac{a_c}{g}$, 6×10^{-2}, was achieved at 15 μl and 7.5 V. This finding indicates that the centrifugal acceleration within the droplet is less significant compared to gravitational acceleration. Furthermore, the correlation between angular velocity and volume suggests that increasing droplet volume further decreases the centrifugal acceleration. Thus, these results support our hypothesis that with appropriate engineering and control, acoustic levitation has the potential to function as a clinostat, effectively simulating microgravity conditions.

5. Conclusions

The initial part of this paper presents the theoretical framework for the shape change and rotational motion of acoustically levitated water droplets using the low-cost non-resonant TinyLev acoustic levitator. Experimental investigations were conducted to examine the impact of applied voltage and droplet volume on the shape (aspect ratio) of the levitated droplet and the rotational motion of the microparticle within it. The results revealed that both applied voltage and droplet volume have a significant influence on the droplet's shape. However, the angular velocity is predominantly affected by the droplet volume rather than the applied voltage.

To assess the microgravity conditions inside the droplet, the ratio between centrifugal acceleration and gravitational acceleration was determined. The functional microgravity achieved by TinyLev was 6×10^{-2}. The experimental results demonstrate the potential of acoustically levitated droplets as a viable option for simulating microgravity on earth

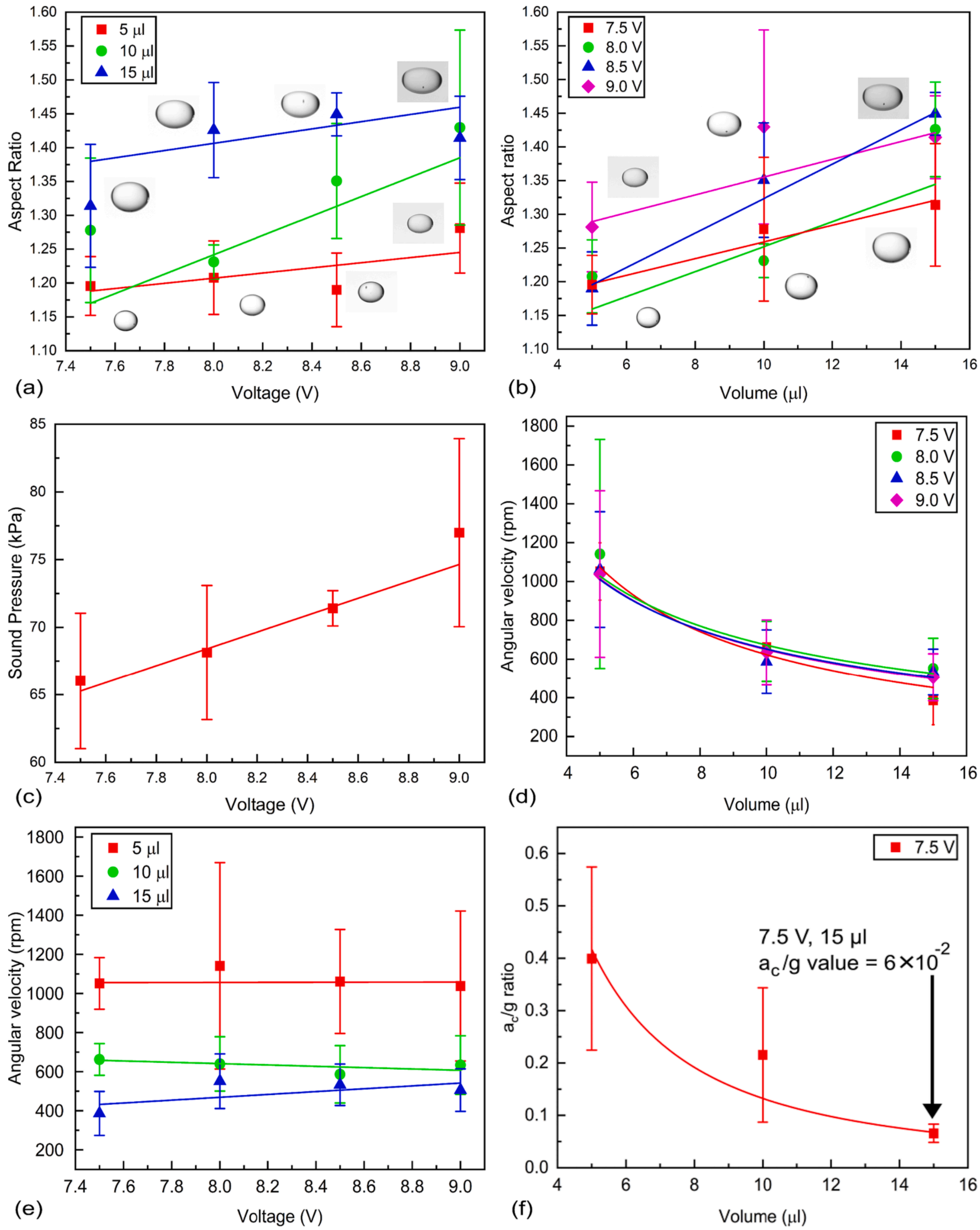

Fig. 3. (a) Variation of aspect ratio of the levitated droplet with applied voltage. (b) Variation of aspect ratio of the droplet with volume. (c) Change in sound pressure with applied voltage. (d) Variation in angular velocity of the levitated droplet with volume. (e) Variation of angular velocity of the levitated droplet with applied voltage. (f) Change in centrifugal acceleration to gravity ratio with volume.

using a clinostat.

Nevertheless, it is important to acknowledge the inherent limitations of the current levitation equipment, particularly in terms of maximum acoustic power generation and droplet volume capacity. The presence of air perturbations poses challenges in maintaining droplet stability and inhibits the ability to sustain microgravity conditions for extended durations. However, based on our current experiment, we hypothesise that a more powerful levitator and careful engineering can lead to improved microgravity conditions within the levitated droplet. Further extensive research in this direction is planned for the future.

CRediT authorship contribution statement

Aditya Vashi: Investigation, Formal analysis, Writing – original draft. **Ajeet Singh Yadav:** Investigation, Software. **Nam-Trung Nguyen:** Project administration, Validation. **Kamalalayam Rajan Sreejith:** Conceptualization, Methodology, Supervision, Validation.

Declaration of Competing Interest

The authors declare the following financial interests/personal relationships which may be considered as potential competing interests:

[Kamalalayam Rajan Sreejith reports financial support was provided by Griffith University.].

Data availability

Data will be made available on request.

Appendix A. Supplementary data

Supplementary data to this article can be found online at https://doi.org/10.1016/j.apacoust.2023.109624.

References

[1] Matsubara T, Takemura K. Containerless bioorganic reactions in a floating droplet by levitation technique using an ultrasonic wave. Adv Sci 2021;8:2002780.
[2] Foresti D, Sambatakakis G, Bottan S, Poulikakos D. Morphing surfaces enable acoustophoretic contactless transport of ultrahigh-density matter in air. Sci Rep 2013;3.
[3] Priego-Capote F, de Castro L. Ultrasound-assisted levitation: lab-on-a-drop. TrAC Trends Anal Chem 2006;25(9):856–67.
[4] Honda K, Fujiwara K, Hasegawa K, Kaneko A, Abe Y, Mixing dynamics of droplets levitated using acoustic tweezers: an optical approach; 2022.
[5] Paradis P-F, Ishikawa T, Lee G-W, Holland-Moritz D, Brillo J, Rhim W-K, et al. Materials properties measurements and particle beam interactions studies using electrostatic levitation. Mater Sci Eng R Rep 2014;76:1–53.
[6] Santesson S, Nilsson S. Airborne chemistry: acoustic levitation in chemical analysis. Anal Bioanal Chem 2004;378(7):1704–9.
[7] Holt RG, Trinh EH. Faraday wave turbulence on a spherical liquid shell. Phys Rev Lett 1996;77:1274–7.
[8] Marx V. Biophysics: using sound to move cells. Nat Methods 2015;12:41–4.
[9] Ashkin A, Dziedzic J. Optical levitation by radiation pressure. Appl Phys Lett 1971; 19:283–5.
[10] Brandt EH. Suspended by sound. Nature 2001;413:474–5.
[11] Jayawant BV. Electromagnetic levitation and suspension techniques; 1981.
[12] Hennet L, Cristiglio V, Kozaily J, Pozdnyakova I, Fischer H, Bytchkov A, et al. Aerodynamic levitation and laser heating. Eur Phys J Special Topics 2011;196: 151–65.
[13] Rhim W-K, Ohsaka K, Paradis P-F, Spjut RE. Noncontact technique for measuring surface tension and viscosity of molten materials using high temperature electrostatic levitation. Rev Sci Instrum 1999;70:2796–801.
[14] Brandt E. Levitation in physics. Science 1989;243:349–55.
[15] Andrade MAB, Pérez N, Adamowski JC. Review of progress in acoustic levitation. Braz J Phys 2018;48:190–213.
[16] Kundt A. Ueber eine neue Art akustischer Staubfiguren und über die Anwendung derselben zur Bestimmung der Schallgeschwindigkeit in festen Körpern und Gasen. Annalen der Physik 1866;203:497–523.
[17] Bruus H. Acoustofluidics 7: The acoustic radiation force on small particles. Lab Chip 2012;12:1014–21.
[18] Ooi CH, Vadivelu R, Jin J, Sreejith KR, Singha P, Nguyen N-K, et al. Liquid marble-based digital microfluidics – fundamentals and applications. Lab Chip 2021;21: 1199–216.
[19] Sreejith KR, Gorgannezhad L, Jin J, Ooi CH, Takei T, Hayase G, et al. Core-Shell beads made by composite liquid marble technology as a versatile microreactor for polymerase chain reaction. Micromachines 2020;11:242.
[20] Yarin A, Pfaffenlehner M, Tropea C. On the acoustic levitation of droplets. J Fluid Mech 1998;356:65–91.
[21] Trinh EH, Hsu CJ. Equilibrium shapes of acoustically levitated drops. J Acoust Soc Am 1986;79:1335–8.
[22] Yamamoto Y, Abe Y, Fujiwara A, Hasegawa K, Aoki K. Internal flow of acoustically levitated droplet. Microgravity Sci Technol 2008;20:277–80.
[23] Hasegawa K, Watanabe A, Kaneko A, Abe Y. Internal flow during mixing induced in acoustically levitated droplets by mode oscillations. Phys Fluids 2019;31:112101.
[24] Watanabe A, Hasegawa K, Abe Y. Contactless fluid manipulation in air: droplet coalescence and active mixing by acoustic levitation. Sci Rep 2018;8:10221.
[25] Hasegawa K, Murata M. Oscillation dynamics of multiple water droplets levitated in an acoustic field. Micromachines 2022;13:1373.
[26] Shen C, Xie W, Wei B. Parametrically excited sectorial oscillation of liquid drops floating in ultrasound. Phys Rev E 2010;81:046305.
[27] Cao H-L, Yin D-C, Guo Y-Z, Ma X-L, He J, Guo W-H, et al. Rapid crystallization from acoustically levitated droplets. J Acoust Soc Am 2012;131:3164–72.
[28] Shi Q, Di W, Dong D, Yap LW, Li L, Zang D, et al. A general approach to free-standing nanoassemblies via acoustic levitation self-assembly. ACS nano 2019;13: 5243–50.
[29] Geng D, Yan N, Xie W, Lü Y, Wei B. Extraordinary solidification mechanism of liquid alloys under acoustic levitation state. Adv Mater 2022;2206464.
[30] Zang D, Li J, Chen Z, Zhai Z, Geng X, Binks BP. Switchable opening and closing of a liquid marble via ultrasonic levitation. Langmuir 2015;31:11502–7.
[31] Vashi A, Sreejith KR, Nguyen NT. Lab-On-a-Chip Technologies for Microgravity Simulation and Space Applications; 2022.
[32] Dedolph RR, Dipert MH. The physical basis of gravity stimulus nullification by clinostat rotation. Plant Physiol 1971;47:756–64.
[33] Marzo A, Barnes A, Drinkwater BW. TinyLev: a multi-emitter single-axis acoustic levitator. Rev Sci Instrum 2017;88:085105.
[34] Gor'kov LP. On the forces acting on a small particle in an acoustical field in an ideal fluid. Sov Phys Dokl 1962:773–5.
[35] O'Neil HT. Theory of focusing radiators. J Acoustical Soc Am 1949;21:516–26.
[36] Rednikov A. Steady streaming around a spherical drop displaced from the velocity antinode in an acoustic levitation field. Quart J Mech Appl Math 2006;59:377–97.
[37] Trinh E, Wang TG. Large-amplitude free and driven drop-shape oscillations: experimental observations. J Fluid Mech 1982;122(-1):315.
[38] Saha A, Basu S, Kumar R. Velocity and rotation measurements in acoustically levitated droplets. Phys Lett A 2012;376:3185–91.
[39] Saha A, Basu S, Kumar R. Particle image velocimetry and infrared thermography in a levitated droplet with nanosilica suspensions. Exp Fluids 2012;52:795–807.
[40] Yan ZL, Xie WJ, Wei B. Vortex flow in acoustically levitated drops. Phys Lett A 2011;375:3306–9.
[41] Marston PL. Shape oscillation and static deformation of drops and bubbles driven by modulated radiation stresses—Theory. J Acoustical Soc Am 1980;67:15–26.
[42] Carl A. Levitate, in; 2017.